NeuroImage 320 (2025) 121477

Contents lists available at ScienceDirect

NeuroImage

journal homepage: www.elsevier.com/locate/ynimg

Cortical aperiodic dynamics in hearing impairments predicts neural tracking of speech

Hangze Mao [a,b,1], Yuhan Lu [c,d,1], Zhuang Jiang [b], Difei Hu [b], Shuihong Zhou [b], Xing Tian [c,d], Yan Han [e,f], Yongtao Xiao [a,**], Zhili Zhang [b,e,*]

[a] School of Medical Technology and Information Engineering, Zhejiang Chinese Medical University, Hangzhou 310053, China
[b] Department of Otorhinolaryngology Head and Neck Surgery, The first affiliated hospital of Zhejiang University School of Medicine, Hangzhou 310009, China
[c] NYU-ECNU Institute of Brain and Cognitive Science, New York University Shanghai, Shanghai 200062, China
[d] Shanghai Frontiers Science Center of Artificial Intelligence and Deep Learning; Division of Arts and Sciences, New York University Shanghai, Shanghai 200122, China
[e] Zhejiang Key Laboratory of Intelligent Rehabilitation and Translational Neuroelectronics, Hangzhou 310053, China
[f] Zhejiang Nurotron Biotechnology Co., Ltd, Hangzhou 310053, China

ARTICLE INFO

Keywords:
Excitation–inhibition balance
Bilateral hearing loss
Single-sided deafness
1/f
Exponent
envelope tracking
Electroencephalography

ABSTRACT

Excitation–inhibition balance is a fundamental property of cortical circuits, reflecting homeostatic plasticity that stabilizes neural activity in the face of functional disruption. This framework has been widely implicated in sensory deprivation and psychiatric disorders. In the auditory domain, it remains unclear how long-term bilateral and unilateral hearing loss reorganizes cortical E-I balance and how such reorganization affects speech processing. Here, we recorded resting-state EEG and measured spectral exponents as a noninvasive proxy for cortical E-I balance in individuals with bilateral hearing loss, single-sided deafness, and normal hearing. We found that spectral exponents differed systematically across hearing loss types. Participants with bilateral hearing loss exhibited reduced exponents, primarily in central-parietal regions, relative to normal-hearing controls, with a gradual increase with prolonged hearing-loss duration. In contrast, left- and right-sided deafness showed distinct patterns of hemispheric lateralization in spectral exponents. Participants also performed a naturalistic speech listening task, allowing quantification of neural tracking of speech. It showed stronger envelope tracking response for bilateral hearing loss group than normal control. Importantly, resting-state exponents across all hearing-impaired groups robustly predicted the strength of speech envelope tracking in noisy environments. These findings reveal dissociable patterns of aperiodic cortical dynamics following bilateral and unilateral auditory deprivation and highlight the homeostatic plasticity in supporting speech perception under challenging listening conditions.

1. Introduction

Excitation–inhibition (E–I) balance is a core neurophysiological mechanism that underlies cognitive processing and has been implicated in both neurodevelopmental and psychiatric disorders (Sohal and Rubenstein, 2019; Sprekeler, 2017; Tao et al., 2014; Yizhar et al., 2011). Importantly, E–I balance is not static but dynamically modulated across the lifespan, behavioral states, and pathological conditions (Chen et al., 2022). It has been hypothesized that when afferent sensory input is reduced, cortical networks shift toward relatively greater excitation to stabilize population activity, reflecting a homeostatic plasticity (Takesian et al., 2009; Turrigiano, 2012; Turrigiano and Nelson, 2004). Supporting this hypothesis, animal studies show that acute auditory deafferentation increases the excitation–inhibition ratio in auditory cortex (Kotak et al., 2005). However, it remains unclear how cortical E–I balance reorganizes over longer timescales in humans, and whether different patterns emerge depending on the laterality of deprivation. Hearing loss provides a natural model to address this question: bilateral hearing loss reduces auditory input globally and has been linked to altered cortical excitability (Kotak et al., 2005), whereas unilateral

* Corresponding author: Department of Otorhinolaryngology Head and Neck Surgery, The first affiliated hospital of Zhejiang University School of Medicine, Hangzhou 310009, China
** Corresponding author at: School of Medical Technology and Information Engineering, Binwen Road 548, Hangzhou 310053, China
E-mail addresses: xyt@zcmu.edu.cn (Y. Xiao), zhangzhili@zju.edu.cn (Z. Zhang).
[1] These authors have contributed equally to this work.

https://doi.org/10.1016/j.neuroimage.2025.121477
Received 13 July 2025; Received in revised form 4 September 2025; Accepted 19 September 2025
Available online 19 September 2025

deafness introduces hemispheric asymmetry and induces asymmetric cortical reorganization (Ponton et al., 2001; Scheffler et al., 1998).

Reductions in peripheral sensory input are thought to shift cortical excitation–inhibition (E–I) balance, thereby altering the gain control and auditory processing (Alain et al., 2022). Magnetic resonance spectroscopy studies show that auditory-cortical GABA levels are reduced in age-related hearing loss and correlate with elevated pure-tone thresholds (Gao et al., 2015; Li et al., 2023; Su et al., 2024). Extending these findings, enhancing GABAergic activity in older adults restored moment-to-moment brain signal variability to levels comparable to young adults (Lalwani et al., 2021). Despite this evidence, it remains unclear whether such E–I indexed alterations manifest in the neural encoding of naturalistic speech, particularly under noisy conditions, and few studies have disentangled the contributions of aging from those of hearing loss.

Resolving these questions requires a noninvasive proxy of cortical E–I balance. Recent work has identified the aperiodic exponent of the EEG power spectrum as such a measure (Donoghue et al., 2020; Gao et al., 2017; Kozma et al., 2024): flatter slopes reflect increased excitation or elevated E/I ratios, whereas steeper slopes indicate greater inhibition. Accumulating evidence links the spectral exponent to various neuropsychiatric conditions—including Alzheimer's disease, epilepsy, and Parkinson's disease—highlighting its clinical relevance (Donoghue, 2024; Pani et al., 2022; Sohal and Rubenstein, 2019). Moreover, because the resting-state exponent and neural speech-tracking response can be derived from EEG recording sessions, it provides a direct bridge between cortical state markers and electrophysiological measures of speech processing.

Here, we investigated how the degree and laterality of hearing loss reshape cortical E–I balance and, in turn, constrain the brain's ability to process naturalistic speech. Using resting-state EEG, we quantified the spectral exponent in age-matched individuals with bilateral hearing loss, left- or right-sided deafness, and normal hearing. Participants also completed a naturalistic speech listening task (Deoisres et al., 2023; Zou et al., 2019). We found that the resting-state spectral exponent systematically varied across hearing loss types and significantly predicted the strength of speech tracking in noisy environments. These findings suggest that bilateral and unilateral hearing loss lead to dissociable alterations in aperiodic cortical dynamics, which in turn shape the neural mechanisms supporting speech perception under real-world listening challenges.

2. Materials and methods

2.1. Participants and audiometry

A total of 156 age-matched subjects participated in this experiment (Table 1). Hearing-impaired (HI; $N = 75$, 36 females), right single-sided deafness (RSSD; $N = 27$, 18 females), left single-sided deafness (LSSD; $N = 27$, 16 females) and normal-hearing (NH; $N = 29$, 21 females) participants between 18 and 60 years of age participated. All participants are right-handed and native Chinese. Two participants (one from the HI group, one from the NH group) were excluded because their exponent values were more than 2.5 standard deviations (SDs) below the group average in the resting-state data. The HI and NH groups were matched in age (HI: mean age 38.6 ± 10.6 (s.d.); NH: mean age 38.3 ± 9.4; $p = 0.854$, two-sided bootstrap). HI participants had symmetrical sensorineural hearing loss, with a pure-tone average (PTA) of 48.8 ± 10.5 dB HL measured at 500, 1000, 2000, and 4000 Hz. For NH participants, the inclusion criterion was audiometric thresholds within 25 dB HL. The RSSD and LSSD groups were matched in age (RSSD: mean age 36.8 ± 10.5; LSSD: mean age 36.9 ± 10.7; $p = 0.989$, two-sided bootstrap). SSD was defined as unilateral hearing loss where the average threshold difference between the two ears was over 50 dB HL, with normal or nearly normal hearing in the better ear (Shang et al., 2020). The PTA for the deaf ear and healthy ear were 107.0 ± 15.1 and 12.7 ± 5.5 dB HL, respectively. Tympanometry and otoscopy screening were conducted to confirm normal middle- and outer-ear function in all participants. They received monetary payment for their participation and the experimental protocol was approved by the Institutional Ethics Review Board of the First Affiliated Hospital of Zhejiang University School of Medicine. Informed consents were obtained from all participants.

Table 1
Demographics and Clinical feature of the participants.

Demographic characteristics	NH group $N = 29$	HI group $N = 75$	RSSD group $N = 27$	LSSD group $N = 27$
Gender, % female (n)	72.4 (21)	48.0 (36)	66.7 (18)	59.3 (16)
Age (yr, mean [SD])	38.3 (9.4)	38.6 (10.6)	36.8 (10.5)	36.9 (10.7)
PTA (dB HL, mean [SD])	14.5 (4.7)	48.8 (10.5)	108.8 (14.1)	105.2 (16.3)
Type of hearing loss	-	Sensorineural	Sensorineural	Sensorineural
Duration (yr, mean [SD])	-	Acquired 6.7 (6.6)	Acquired 14.7 (11.1)	Acquired 11.8 (10.5)
Etiology (n)				
Sudden onset	-	1	7	5
Ototoxic medication	-	2	1	0
Genetic factors	-	2	0	0
Infection	-	1	0	0
Other diseases	-	0	2	3
Unknown origin	-	69	17	19
Hearing aid or cochlear implant use	-	None	None	None

N, number; yr, year; PTA, pure-tone average (mean of thresholds at 500, 1000, 2000, and 4000 Hz); dB, decibel; HL, hearing level.

2.2. Stimuli and procedures

The speech stimulus was excerpted from a narration of the story *Thatched Memories* by Wenxuan Cao. Eight segments of recording were used in the experiment, each lasting approximately four minutes and constrained to end at a sentence boundary. All segments were normalized to the same intensity, measured by the root mean square (RMS). Half of the speech segments (N = 4) were presented in a quiet listening environment (no noise added in), while the other half were mixed with four-talker babble noise (signal-to-noise ratio = 0 dB), measured by RMS. The target speech was presented at an individually adjusted intensity to avoid large variations in speech intelligibility across participants. The sound field was first calibrated with a measurement microphone, and participants then adjusted the level of two 10-s speech samples to a comfortable intensity. The resulting individual levels were used for stimulus presentation (NH: 63.21 ± 2.79 dB SPL; left SSD: 63.33 ± 3.10 dB; right SSD: 64.81 ± 4.04 dB; bilateral HI: 69.79 ± 4.26 dB; **Fig. S1**).

EEG experiments were performed in a double-walled, electrically shielded sound-attenuating booth. Participants were presented with a resting-state task followed by a speech-comprehension task. For resting state task, participants were asked to comfortably seated and had a two-minute eyes-closed resting-state EEG recording. For the speech-comprehension task, they were instructed to maintain eye fixation on a black cross presented on a computer screen. They received eight segments (i.e., four segments of clear speech and four segments of speech in babble noise) of stories through a loudspeaker placed one meter away from participants and roughly kept the same height of participants' ears. The presentation order of the stimulus was kept the same across all participants, with the quiet condition preceding the noise condition. The participants were asked two multiple-choice comprehension questions (each with four options) after each segment to ensure their attention. Under the quiet condition, groups NH, HI, RSSD, and LSSD participants achieved average accuracies of 94.6 ± 10.3%, 92.9 ± 10.5%, 96.3 ±

7.5%, and 93.1 ± 10.4%, respectively; under the noise condition, their accuracies were 91.5 ± 10.6%, 72.5 ± 26.1%, 94.0 ± 9.8%, and 88.0 ± 15.0%, respectively. Before EEG recording, audiometry assessment and Montreal Cognitive Assessment (MoCA) were performed for each participant.

2.3. EEG recording and preprocessing

Resting-state and task EEG data were acquired using a 128-channel Neuroscan system (Compumedics-Neuroscan, Charlotte, NC, USA), sampled at 1,000 Hz. Four channels were used to record horizontal and vertical electrooculograms (EOG) and EOG artifacts were removed using the least squares regression method (Ding et al., 2017). EEG signals were re-referenced offline to the average of all electrodes. For the speech-compensation task, both the EEG data and the speech envelopes were down-sampled to 100 Hz, and the EEG data was then band-pass filtered between 1 and 8 Hz using a linear-phase finite impulse response (FIR) filter to extract EEG envelope. For resting-state task, EEG data was down-sampled to 250 Hz and was filtered between 1 and 40 Hz.

2.4. Spectral exponent analysis

Spectral exponent of resting-state EEG recordings was estimated using FOOOF algorithm (Donoghue et al., 2020). First, spectra were calculated for each channel, using Welch's method (2-s windows, 80% overlap) and the slope of the aperiodic component of the spectra was automatically estimated using FOOOF. Settings for the algorithm were set as: peak width limits: [1-6]; max number of peaks: 3; minimum peak height: 0.05; peak threshold: 1.5; and aperiodic mode: 'knee'. The selection of the aperiodic mode, which modeled the aperiodic component with a Lorentzian-shaped function, was based on visual inspection of the spectra. Two independent raters (Y.L. and H.M.) consistently judged the knee mode to provide a better fit across participants compared with the fixed mode, which applied a 1/f-like curve (**Fig. S2**). Electrodes with poor model fits (fit error < 0.9) were excluded from further analysis (McKeown et al., 2025), with a median of 4.5 electrodes (IQR: 1.0-14.5) removed per participant. For SSD participants, we calculated the lateralization index of the spectral exponent. The index was computed as (L – R) / (L + R), where L and R represent the mean spectral exponent across electrodes over the left and right hemispheres, respectively.

2.5. Temporal response function

To assess the relationship between the neural response and the presented speech stimuli, a linear temporal response function (TRF) was estimated between the stimulus and the response (Wang et al., 2025). The TRF was independently computed for each model and each participant using ridge regression with 10-fold cross-validation (Zou et al., 2019). The TRF was estimated using least squares with L2 regularization. The regularization parameter was optimized to maximize predictive power, which was measured by the correlation between predicted and actual neural responses. Specifically, the regularization parameter ranged from 0 to 0.1, and 0.001 was determined as the optimal value as it yielded the highest predictive power averaged across conditions and participants. The two major peaks of the TRF have latencies near 50 ms and 150 ms. Only the 150 ms peak, which was dominant and exhibited a robust amplitude, was included in the subsequent analyses, identified by the RMS of the EEG response across electrodes between 100 and 200 ms.

3. Statistical analysis

The bootstrap significance test was conducted using a bias-corrected and accelerated procedure (Efron and Tibshirani, 1994). In this procedure, the data from all participants were resampled 10,000 times with replacement, and for each resample, the data were averaged across participants, yielding a total of 10,000 mean values. For paired comparisons (e.g., comparisons of exponent between hemispheres), a bootstrap test was performed to test the differences; If N_S out of the 10,000 mean values were greater (or smaller) than 0, the significance level was calculated as N_S/10,000. For between-subject comparisons (e.g., comparisons among NH, HI, RSSD and LSSD groups), data (e.g., exponent, TRF and predictive power) from the participants were resampled to estimate the null distribution. If the mean value across one group was greater (or smaller) than N_S out of the 10,000 resampled mean values of the other group, the significance level was calculated as N_S/10,000. When multiple comparisons were conducted, p-values were further adjusted using the false discovery rate (FDR) correction (Benjamini and Hochberg, 1995).

In the neural tracking analysis, chance-level predictive power was estimated by generating surrogate neural responses. Each surrogate response was created by circularly shifting the actual neural response by a time lag ranging from 100 to 300 seconds in 2-second increments. This procedure resulted in 101 surrogate neural responses. If the actual predictive power exceeded the 95% percentile of the chance-level predictive power, it was considered statistically significant ($p < 0.05$).

We investigated the effect of hearing impairment on exponent by means of a linear mixed effect model (LME) using maximum likelihood estimation with MATLAB's fitlme function. The fixed effects in the LME included the predictors of interest, while the random effects accounted for variability across participants. All significant effects are reported in the results section, including the β estimates and test statistics (p-values). We performed a Spearman correlation analysis to assess the linear relation between exponent and neural envelope tracking (i.e., TRF and predictive power).

4. Results

4.1. Resting-state spectral exponent in normal-hearing and bilateral hearing-impaired participants

EEG recordings during resting state in hearing-impaired (HI) and normal-hearing (NH) participants (N = 74 and 28, respectively) were transformed into power spectral density (PSD) estimates in log-log space, revealing a characteristic 1/f-like distribution (Fig. 1A, black lines). To isolate the aperiodic background activity from oscillatory peaks, we applied a Lorentzian fit, separating the 1/f component (blue line) from narrowband oscillations (red dashed line). The slope of the aperiodic component—termed the spectral exponent (black dashed line)—quantified the decay rate of spectral power: higher exponents indicated steeper decline and stronger low-frequency dominance, while lower values reflected flatter spectra. The spectral exponent exhibited a centro-parietal topography in both groups (Fig. 1B). Channel-wise comparisons revealed significantly higher exponents in NH participants than HI participants over large-scale parieto-occipital regions ($p <$ 0.05, two-sided bootstrap, FDR uncorrected), especially for the centro-parietal ROI ($p = 0.029$ for channels in red pentagon, two-sided bootstrap; Fig. 1C). To identify potential factors contributing to altered exponents in the HI group, we constructed a linear mixed-effects model. Among predictors, only the duration of hearing loss showed a significant positive association with the exponent ($t(67) = 2.41$, $p = 0.019$, one-sample t-test; Fig. 1D), suggesting that longer durations of auditory deprivation may be associated with compensatory cortical dynamics changes reflected in the spectral exponent.

4.2. Resting-state exponent predicts neural tracking of speech in noise

Next, we investigated whether spectral exponent of HL participants during resting state can predict cortical processing of continuous speech. In both clear-speech and speech-in-noise conditions, we employed the TRF to access how the speech envelope was encoded in the EEG activity (Fig. 2A). We first evaluated the predictive power of TRF, defined as the correlation between the TRF model prediction and EEG measurement.

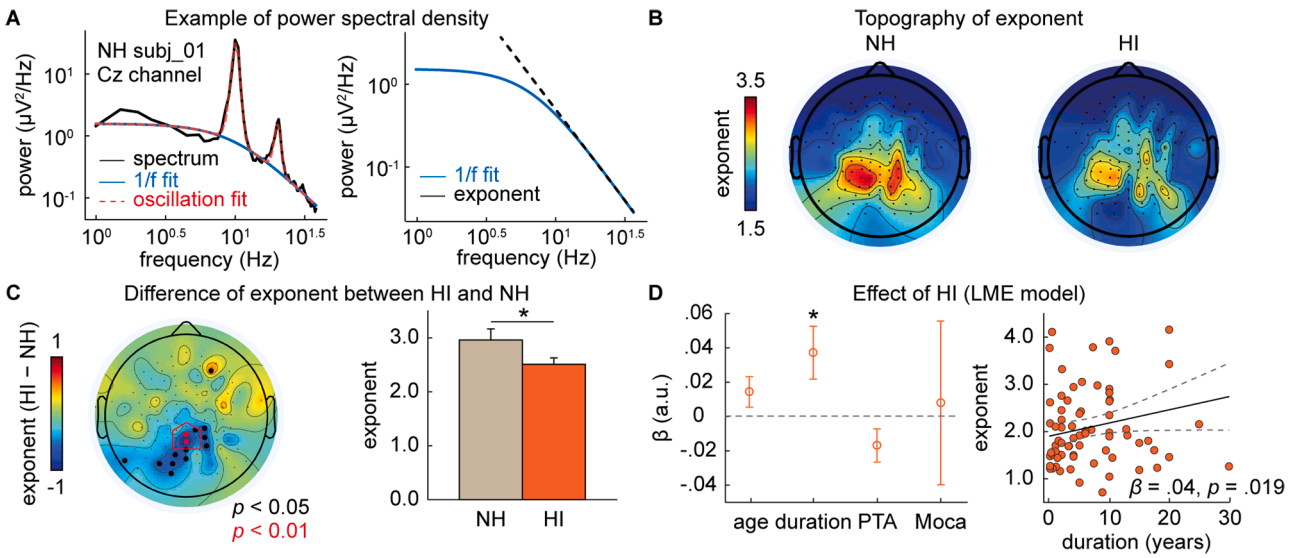

Fig 1. Resting-state spectral exponent in normal-hearing and bilateral hearing-impaired participants. A, An example of PSD at single EEG channels. Original spectrum can be decomposed into aperiodic (shown as blue line) and periodic components (red dashed line) by using FOOOF algorithm (see Methods). **B**, Spectral exponent in both NH and HI participants shows a centro-parietal distribution. **C**, Exponent in NH participants is larger than that in HI participants at the EEG channels over centro-parietal regions (the topography shows the HI − NH values). Red and black dots denote $p < 0.01$ and 0.05. Bar plot shows an averaged exponent across channels over the centro-parietal region (red pentagon). **D**, The effects of age, duration of hearing loss, pure-tone threshold, and MoCA cognitive score on exponent are revealed by a generalized linear mixed-effect model. Regression coefficients for each predictor are extracted from the model. The duration of hearing loss exerts a significant positive effect on spectral exponent. In **C** and **D**, error bars denote the standard error of mean (SEM) across participants. *$p < 0.05$.

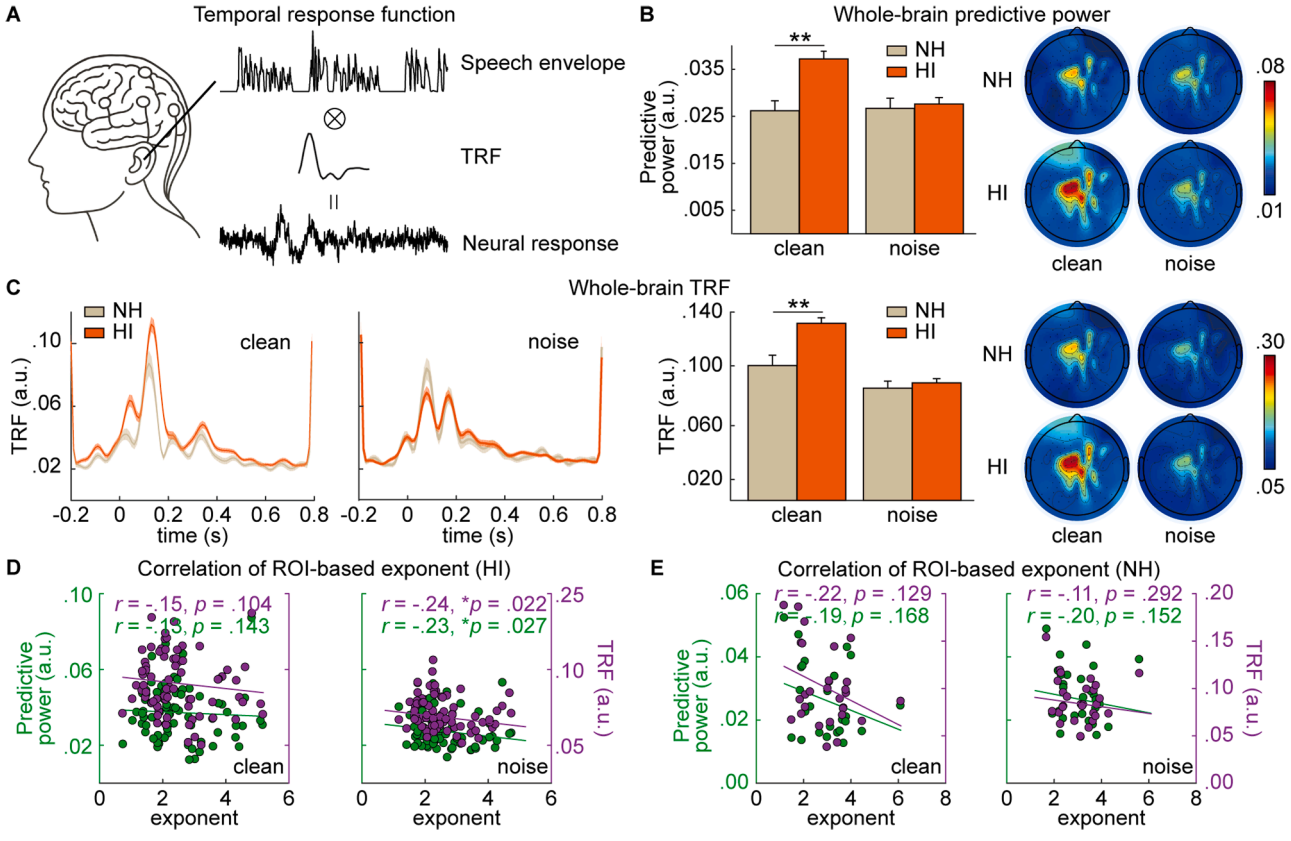

Fig 2. Resting-state spectral exponent in bilateral hearing-impaired participants predicts neural tracking of speech in noise. A, Schematic of the TRF approach. TRF models the mapping between the speech envelope and EEG signals to assess time-locked neural tracking of speech envelope. **B**, Group-level comparisons of TRF predictive power in clean and noise conditions. HI participants show significantly stronger responses than NH participants in the clean condition, but no group difference is found under noise. EEG topography on the right panels shows central distributions of predictive power and TRF amplitude. **C**, TRF waveforms in clean (left) and noise (right) conditions. Shaded areas indicate SEM across participants. **D** and **E**, resting-state spectral exponent averaged over centro-parietal regions significantly correlated with both TRF predictive power (green) and amplitude (purple) during speech-in-noise, in HI participants (**D**), but not in NH participants (**E**). *$p < 0.05$, **$p < 0.005$.

The predictive power was above chance level for all conditions ($p < 0.05$; Fig. 2B). HI participants exhibited significantly greater TRF predictive power than NH participants during the clean-speech condition ($p = 0.0002$, two-sided bootstrap, FDR corrected), but no group difference was observed during the speech-in-noise condition ($p = 0.784$, two-sided bootstrap, FDR corrected). Consistently, TRF amplitude—reflecting the strength of EEG responses to the speech envelope—was also higher in HI than NH participants during the clean-speech condition ($p = 0.002$, two-sided bootstrap, FDR corrected; Fig. 2C), but no difference emerged under speech-in-noise condition ($p = 0.628$, two-sided bootstrap, FDR corrected). Importantly, we assessed whether the resting-state spectral exponent averaged over centro-parietal electrodes (defined in Fig. 1D), the significant region differentiated HI and NH participants, predicted individual TRF performance. In HI participants, a smaller exponent (i.e., flatter spectrum) was significantly associated with stronger TRF performance during the speech-in-noise condition, as indicated by both predictive power and TRF amplitude ($r = -0.23$ and -0.24, $p = 0.027$ and 0.022, respectively, Spearman r; Fig. 2D). No such relationships were observed in NH participants (Fig. 2E). These results suggested that the spectral exponent over centro-parietal regions may serve as a marker of cortical plasticity that predicted speech tracking under challenging listening conditions in individuals with bilateral hearing loss.

4.3. Lateralized spectral exponent in left- and right-sided deafness

To examine whether the absence of auditory input from the left versus right ear differentially influenced large-scale cortical aperiodic dynamics, we compared the spectral exponent across EEG channels between participants with LSSD and RSSD ($N = 27$ for both groups). The aperiodic component of the power spectrum showed a higher exponent (i.e., a steeper spectral slope) in RSSD compared to LSSD participants ($p = 0.015$, two-sided bootstrap; Fig. 3A). To rule out the influence of other individual differences that might contribute to this group-level effect, we constructed a LME model with group (LSSD vs. RSSD), age, duration of hearing loss, pure-tone average threshold, and MoCA scores as fixed effects. Among all predictors, only the group factor significantly explained the variance in whole-brain exponent values ($t(48) = -3.50$, $p = 0.001$, one-sample t-test; Fig. 3B), indicating that the side of deafness alone accounts for the observed spectral differences. Building on this group-level effect, we next asked whether spectral exponent may also differ between hemispheres, given the unilateral reduction in auditory input. In LSSD participants, the exponent tended to be higher over left-hemispheric electrodes compared to right-hemispheric electrodes ($p = 0.087$, two-sided bootstrap, FDR corrected; Fig. 3C), an effect not observed in RSSD participants ($p = 0.564$, two-sided bootstrap, FDR corrected). To quantitatively capture this asymmetry, we computed a lateralization index (LI) for each participant (Fig. 3D), laying the foundation for examining whether the LI induced by the side of deafness can predict cortical encoding of continuous speech.

4.4. Lateralized spectral exponent changes predict neural tracking of speech in noise

Next, we investigated cortical tracking of the speech envelope in SSD participants, characterized by unilateral deafness with the other ear retaining normal hearing. Both TRF amplitude (Fig. 4A) and predictive power (Fig. 4B) were comparable between left-sided and right-sided SSD, in both clear-speech and speech-in-noise conditions ($p > 0.108$, two-sided bootstrap, FDR corrected), and exhibited central distributions (right panels). To further elucidate the relationship between resting-state aperiodic dynamics and speech processing, we analyzed correlations between the LI of the spectral exponent and TRF measures. Under the speech-in-noise condition, the LI significantly predicted predictive power and TRF amplitude ($r = -0.39$ and -0.37, $p = 0.022$ and 0.030, respectively, Spearman r; Fig. 4C) in RSSD participants. In LSSD participants, we observed a positive trend for both predictive power and TRF amplitude ($r = 0.26$ and 0.36, $p = 0.094$ and 0.034, respectively, Spearman r; Fig. 4C). Notably, no significant correlations emerged under the clean-speech condition for either participant group (Fig. 4D).

5. Discussion

In this study, we examined how E-I balance, indexed by the spectral exponent of resting-state EEG, are altered in individuals with bilateral hearing loss and those with unilateral deafness. We found that individuals with bilateral hearing loss exhibited reduced spectral exponents compared to normal-hearing controls, indicating a flatter aperiodic slope. Notably, the exponent increased as a function of hearing loss duration, suggesting compensatory cortical reorganization over time. In participants with single-sided deafness, spectral exponents differed significantly between those with left versus right hemispheres, revealing asymmetric changes in large-scale cortical dynamics. Importantly, in both hearing-impaired groups, spatial variations in the spectral exponent predicted the strength of neural tracking of speech in noise, highlighting its potential as a biomarker for auditory cortical plasticity.

5.1. Spectral exponent in bilateral hearing loss

Individuals with bilateral hearing impairment exhibited significantly reduced spectral exponents compared to normal-hearing controls, particularly over centro-parietal regions (Fig. 1C). A flatter aperiodic slope implies reduced dominance of low-frequency activity and relatively elevated high-frequency power, a spectral profile commonly interpreted as a macroscale signature of increased cortical excitation or diminished inhibition (Brake et al., 2024; Donoghue et al., 2020; Gao et al., 2017; Lendner et al., 2020). Animal studies have consistently shown that acute auditory deafferentation, such as cochlear ablation,

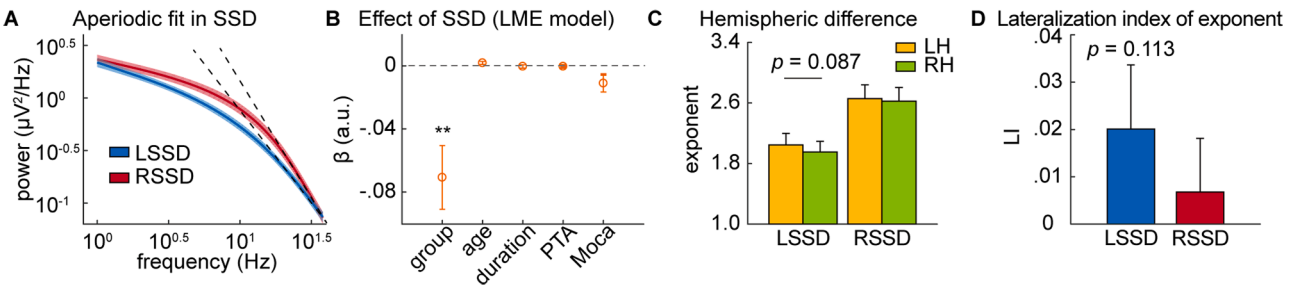

Fig 3. Lateralized exponent in single-sided deafness predicts neural tracking of speech in noise. A, Spectral aperiodic activity averaged across participants shows a larger exponent for RSSD participants than LSSD participants. **B**, Generalized LME model confirms the effect of sided deafness, but not for other individual factors. **C**, LSSD participants have larger exponent in the left-hemispheric electrodes than the right-hemispheric electrodes, showing a left-lateralized exponent. **D**, Lateralization index was calculated as (L - R)/(L + R) for each participant, where L and R represent the mean spectral exponent across electrodes in the left and right hemispheres (excluding electrodes along the midline). $^{**}p < 0.005$.

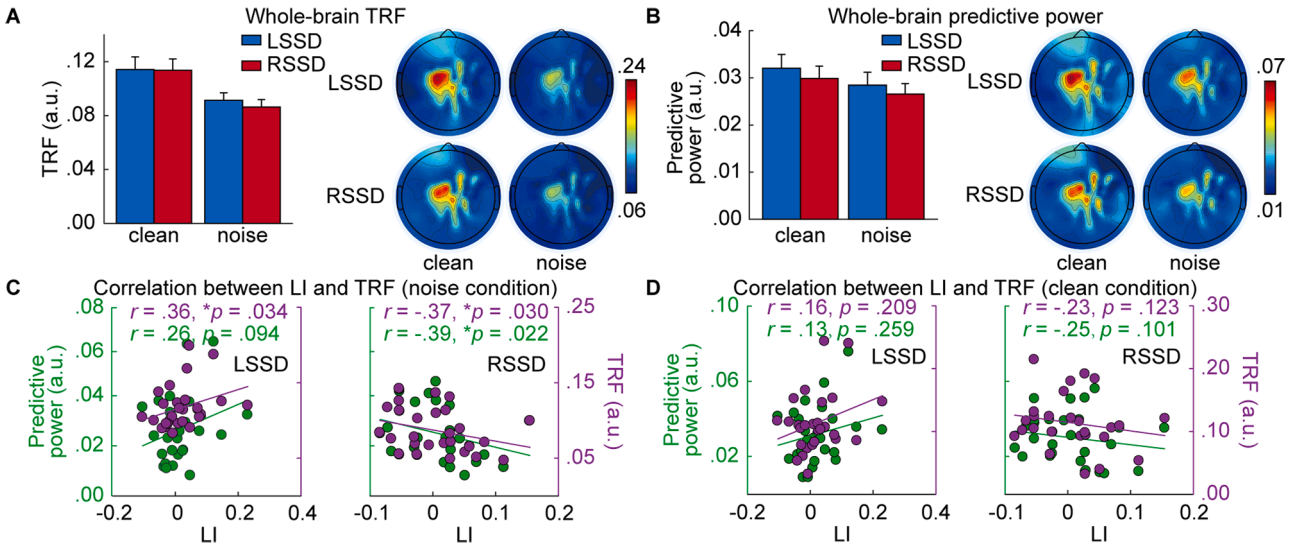

Fig 4. Cortical tracking of speech envelope in SSD participants. A and **B**, Amplitude and predictive power of TRF in LSSD and RSSD participants during clean speech and speech-in-noise conditions, with topographies showing spatial distributions. **C** and **D**, Correlations between the lateralization index (LI) of spectral exponent and neural tracking measures (TRF predictive power and amplitude) in (**C**) speech-in-noise and (**D**) clean speech conditions. Scatter plots denote individual participants. $^*p < 0.05$.

rapidly reduces GABA-mediated inhibition and elevates cortical excitability, thereby flattening the spectral slope (Chen et al., 2022; Kotak et al., 2005). Interestingly, we observed that the spectral exponent gradually increased with the duration of hearing loss, suggesting a progressive normalization of cortical excitation-inhibition balance over time. Supporting this finding, previous research indicates that inhibitory plasticity mechanisms, including synaptic scaling, interneuron sprouting, and thalamo-cortical reorganization, operate over months to years, incrementally restoring inhibitory tone in response to sustained auditory deprivation (Herrmann and Butler, 2021; Sanes, 2013; Takesian et al., 2009, 2012).

5.2. *Spectral exponent in single-sided deafness*

It is well established that auditory input from each ear projects predominantly to the contralateral auditory cortex, with weaker ipsilateral projections (Kaas and Hackett, 2000; Tervaniemi and Hugdahl, 2003). In individuals with single-sided deafness, this asymmetric pathway results in an imbalance of auditory input between the hemispheres: greater input to the hemisphere contralateral to the intact ear and severely reduced input to the contralateral hemisphere of the deaf ear. This asymmetry in sensory drive may underlie cortical reorganization and lateralized changes in neural dynamics observed in SSD (Balaram et al., 2019; Sharma et al., 2016). In our study, participants with left-sided deafness exhibited overall lower spectral exponents, but showed a clear leftward lateralization—specifically, larger exponents in the left than the right hemisphere—suggesting a stronger E-I balance in the right hemisphere. A plausible explanation may involve hemispheric specialization, particularly the left hemisphere's dominant role in processing speech and language (Hickok and Poeppel, 2007; Peelle, 2012). In left-sided deafness, the reduced input to the right auditory cortex may lead to increased cortical excitability or reduced inhibition, resulting in a lower spectral exponent in that hemisphere and thus leftward lateralization. In contrast, right-sided deafness reduces input to the left auditory and language-dominant cortex, but does not lead to significant lateralization, possibly due to different mechanisms of functional compensation. Our findings suggest that unilateral auditory deprivation induces asymmetric cortical adaptations that reflect underlying hemispheric specialization.

5.3. *Resting-state spectral exponent predicts auditory processing*

It is well-established that low-frequency neural activity can track speech across multiple timescales, from acoustic features (Khalighinejad et al., 2017; Lesenfants et al., 2019; Rimmele et al., 2015) to linguistic structures (Jin et al., 2020; Lu et al., 2023; Lu et al., 2022). Among these, envelope tracking has been most widely studied and shown to correlate with behavioral performance in speech comprehension (Decruy et al., 2020; Van Hirtum et al., 2023). A number of factors, including stimulus intensity, can influence the strength of this response. Previous EEG studies with clear speech typically report prediction accuracies ranging from 0.02 to 0.10 (Drennan and Lalor, 2019; Fuglsang et al., 2020; Reetzke et al., 2021; Verschueren et al., 2022), which is consistent with the magnitude observed in the present study. Across studies, stimulus intensity has been controlled in different ways, such as subjective adjustments or fixed levels above hearing thresholds (Decruy et al., 2020; Fuglsang et al., 2020; Puschmann et al., 2019). Regardless of the method, a consistent finding is that hearing-impaired listeners exhibit enhanced envelope tracking compared with normal-hearing controls. Our results align with this pattern, indicating that the stronger tracking in the HI group cannot be attributed solely to intensity differences. This enhancement likely reflects compensatory neural mechanisms. Hearing loss may trigger increased top-down gain control from higher-order cortical regions, boosting the neural representation of degraded input (Alain et al., 2022; Du et al., 2016). The current study suggests that enhanced envelope tracking in hearing-impaired listeners reflects cortical adaptation linked to shifts in excitation–inhibition balance (Campbell and Sharma, 2013; Gao et al., 2017).

Accumulating evidence indicates that the spectral exponent, a measure reflecting the balance between neural excitation and inhibition, is closely associated with various neurological and psychiatric conditions, capturing fundamental changes in cortical dynamics as observed through EEG and MEG recordings (Donoghue et al., 2020; Voytek et al., 2015). Extending this framework into auditory neuroscience, we show that spectral exponent alterations induced by hearing impairment can be significantly correlated with auditory processing abilities, specifically evaluated through neural envelope tracking tasks. Envelope tracking response provides a robust neural index of cortical encoding of speech envelope features (Ding et al., 2014; Ding and Simon, 2012, 2013; Presacco et al., 2016). In the context of hearing loss, previous studies have demonstrated stronger neural tracking of speech envelopes in

hearing impaired participants compared with normal hearing, suggesting compensated cortical representation of speech envelope (Fuglsang et al., 2020; Millman et al., 2017; Petersen et al., 2017). Our results further establish that the spectral exponent specifically predicts auditory processing performance in speech-in-noise conditions rather than clear speech conditions. Speech-in-noise processing involves more complex neural computations and places greater demands on cortical inhibitory-excitatory balance, which is sensitively reflected by changes in the spectral exponent (Alain et al., 2014; Parthasarathy et al., 2020). Consequently, this predictive relationship underscores the spectral exponent as a fundamental neural signature reflecting cortical dynamics crucial for robust auditory perception, particularly under challenging listening scenarios commonly encountered in daily life.

In conclusion, the present study revealed dissociable patterns of spectral exponents—an index of cortical E-I balance—across bilateral and unilateral hearing loss. Importantly, resting-state spectral exponents reliably predicted the strength of neural tracking responses to speech in noise, highlighting a functional link between spontaneous cortical dynamics and sensory processing. These findings suggest that peripheral auditory deprivation drives distinct forms of cortical reorganization depending on the type and duration of hearing loss. More broadly, our results underscore the utility of the aperiodic exponent as a noninvasive biomarker of cortical state and its potential relevance for understanding compensatory mechanisms in sensory-impaired populations.

Data and code availability statement

The code used for data analysis in this study is available at Mendeley Data (DOI: 10.17632/wcrsy9fs3z.1). De-identified patient data are available from the corresponding author upon reasonable request, subject to institutional and ethical approvals.

Funding sources

This study was supported by the National Natural Science Foundation of China 82201276; “Pioneer” and “Leading Goose” R&D Program of Zhejiang 2025C01108.

Ethics statement

This work was approved by the Institutional Ethics Review Board of the First Affiliated Hospital of Zhejiang University School of Medicine (Approval No: 2023-0606). Potential consequences and benefits were explained, and written informed consent was obtained from each subject before this study.

CRediT authorship contribution statement

Hangze Mao: Writing – original draft, Data curation, Conceptualization. **Yuhan Lu:** Writing – review & editing, Writing – original draft, Data curation. **Zhuang Jiang:** Writing – review & editing, Data curation, Conceptualization. **Difei Hu:** Data curation, Conceptualization. **Shuihong Zhou:** Supervision. **Xing Tian:** Writing – review & editing, Supervision. **Yan Han:** Supervision. **Yongtao Xiao:** Supervision. **Zhili Zhang:** Writing – review & editing, Supervision, Conceptualization.

Declaration of competing interest

None

Acknowledgments

We thank Linyang Qian, Yangyang Yu, and Qinlei Guo for their assistance on data collection.

Supplementary materials

Supplementary material associated with this article can be found, in the online version, at doi:10.1016/j.neuroimage.2025.121477.

Data availability

Data will be made available on request.

References

Alain, C., Chow, R., Lu, J., Rabi, R., Sharma, V.V., Shen, D., Anderson, N.D., Binns, M., Hasher, L., Yao, D., 2022. Aging enhances neural activity in auditory, visual, and somatosensory cortices: the common cause revisited. J. Neurosci. 42, 264–275.
Alain, C., Roye, A., Salloum, C., 2014. Effects of age-related hearing loss and background noise on neuromagnetic activity from auditory cortex. Front. Syst. Neurosci. 8, 8.
Balaram, P., Hackett, T., Polley, D., 2019. Synergistic transcriptional changes in AMPA and GABAA receptor genes support compensatory plasticity following unilateral hearing loss. Neuroscience 407, 108–119.
Benjamini, Y., Hochberg, Y., 1995. Controlling the false discovery rate: a practical and powerful approach to multiple testing. J. R. Stat. Soc.: Series B (Methodological) 57, 289–300.
Brake, N., Duc, F., Rokos, A., Arseneau, F., Shahiri, S., Khadra, A., Plourde, G., 2024. A neurophysiological basis for aperiodic EEG and the background spectral trend. Nat. Commun. 15, 1514.
Campbell, J., Sharma, A., 2013. Compensatory changes in cortical resource allocation in adults with hearing loss. Front. Syst. Neurosci. 7, 71.
Chen, L., Li, X., Tjia, M., Thapliyal, S., 2022. Homeostatic plasticity and excitation-inhibition balance: The good, the bad, and the ugly. Curr. Opin. Neurobiol. 75, 102553.
Decruy, L., Vanthornhout, J., Francart, T., 2020. Hearing impairment is associated with enhanced neural tracking of the speech envelope. Hear. Res. 393, 107961.
Deoisres, S., Lu, Y., Vanheusden, F.J., Bell, S.L., Simpson, D.M., 2023. Continuous speech with pauses inserted between words increases cortical tracking of speech envelope. PLoS. One 18, e0289288.
Ding, N., Chatterjee, M., Simon, J.Z., 2014. Robust cortical entrainment to the speech envelope relies on the spectro-temporal fine structure. Neuroimage 88, 41–46.
Ding, N., Melloni, L., Yang, A., Wang, Y., Zhang, W., Poeppel, D., 2017. Characterizing neural entrainment to hierarchical linguistic units using electroencephalography (EEG). Front. Hum. Neurosci. 11, 481.
Ding, N., Simon, J.Z., 2012. Emergence of neural encoding of auditory objects while listening to competing speakers. Proc. Natl. Acad. Sci. 109, 11854–11859.
Ding, N., Simon, J.Z., 2013. Adaptive temporal encoding leads to a background-insensitive cortical representation of speech. J. Neurosci. 33, 5728–5735.
Donoghue, T., 2024. A systematic review of aperiodic neural activity in clinical investigations. medRxiv. 2024.2010. 2014.24314925.
Donoghue, T., Haller, M., Peterson, E.J., Varma, P., Sebastian, P., Gao, R., Noto, T., Lara, A.H., Wallis, J.D., Knight, R.T., 2020. Parameterizing neural power spectra into periodic and aperiodic components. Nat. Neurosci. 23, 1655–1665.
Drennan, D.P., Lalor, E.C., 2019. Cortical tracking of complex sound envelopes: modeling the changes in response with intensity. eNeuro 6.
Du, Y., Buchsbaum, B.R., Grady, C.L., Alain, C., 2016. Increased activity in frontal motor cortex compensates impaired speech perception in older adults. Nat. Commun. 7, 12241.
Efron, B., Tibshirani, R.J., 1994. An introduction to the bootstrap. Chapman and Hall/CRC.
Fuglsang, S.A., Märcher-Rørsted, J., Dau, T., Hjortkjær, J., 2020. Effects of sensorineural hearing loss on cortical synchronization to competing speech during selective attention. J. Neurosci. 40, 2562–2572.
Gao, F., Wang, G., Ma, W., Ren, F., Li, M., Dong, Y., Liu, C., Liu, B., Bai, X., Zhao, B., 2015. Decreased auditory GABA+ concentrations in presbycusis demonstrated by edited magnetic resonance spectroscopy. Neuroimage 106, 311–316.
Gao, R., Peterson, E.J., Voytek, B., 2017. Inferring synaptic excitation/inhibition balance from field potentials. Neuroimage 158, 70–78.
Herrmann, B., Butler, B.E., 2021. Hearing loss and brain plasticity: the hyperactivity phenomenon. Brain Struct. Funct. 226, 2019–2039.
Hickok, G., Poeppel, D., 2007. The cortical organization of speech processing. Nat. Revi. Neurosci. 8, 393–402.
Jin, P., Lu, Y., Ding, N., 2020. Low-frequency neural activity reflects rule-based chunking during speech listening. Elife 9, e55613.
Kaas, J.H., Hackett, T.A., 2000. Subdivisions of auditory cortex and processing streams in primates. Proc. Natl. Acad. Sci. 97, 11793–11799.
Khalighinejad, B., da Silva, G.C., Mesgarani, N., 2017. Dynamic encoding of acoustic features in neural responses to continuous speech. J. Neurosci. 37, 2176–2185.
Kotak, V.C., Fujisawa, S., Lee, F.A., Karthikeyan, O., Aoki, C., Sanes, D.H., 2005. Hearing loss raises excitability in the auditory cortex. J. Neurosci. 25, 3908–3918.
Kozma, C., Schroeder, G., Owen, T., de Tisi, J., McEvoy, A.W., Miserocchi, A., Duncan, J., Wang, Y., Taylor, P.N., 2024. Identifying epileptogenic abnormality by decomposing intracranial EEG and MEG power spectra. J. Neurosci. Methods 408, 110180.
Lalwani, P., Garrett, D.D., Polk, T.A., 2021. Dynamic recovery: GABA agonism restores neural variability in older, poorer performing adults. J. Neurosci. 41, 9350–9360.

Lendner, J.D., Helfrich, R.F., Mander, B.A., Romundstad, L., Lin, J.J., Walker, M.P., Larsson, P.G., Knight, R.T., 2020. An electrophysiological marker of arousal level in humans. Elife 9, e55092.
Lesenfants, D., Vanthornhout, J., Verschueren, E., Decruy, L., Francart, T., 2019. Predicting individual speech intelligibility from the cortical tracking of acoustic-and phonetic-level speech representations. Hear. Res. 380, 1–9.
Li, N., Ma, W., Ren, F., Li, X., Li, F., Zong, W., Wu, L., Dai, Z., Hui, S.C., Edden, R.A., 2023. Neurochemical and functional reorganization of the cognitive-ear link underlies cognitive impairment in presbycusis. Neuroimage 268, 119861.
Lu, Y., Jin, P., Ding, N., Tian, X., 2023. Delta-band neural tracking primarily reflects rule-based chunking instead of semantic relatedness between words. Cerebral Cortex 33, 4448–4458.
Lu, Y., Jin, P., Pan, X., Ding, N., 2022. Delta-band neural activity primarily tracks sentences instead of semantic properties of words. Neuroimage 251, 118979.
McKeown, D.J., Roberts, E., Finley, A.J., Kelley, N.J., Keage, H.A., Schinazi, V.R., Baumann, O., Moustafa, A.A., Angus, D.J., 2025. Lower aperiodic EEG activity is associated with reduced verbal fluency performance across adulthood. Neurobiol. Aging 151, 29–41.
Millman, R.E., Mattys, S.L., Gouws, A.D., Prendergast, G., 2017. Magnified neural envelope coding predicts deficits in speech perception in noise. J. Neurosci. 37, 7727–7736.
Pani, S.M., Saba, L., Fraschini, M., 2022. Clinical applications of EEG power spectra aperiodic component analysis: A mini-review. Clin. Neurophysiol. 143, 1–13.
Parthasarathy, A., Hancock, K.E., Bennett, K., DeGruttola, V., Polley, D.B., 2020. Bottom-up and top-down neural signatures of disordered multi-talker speech perception in adults with normal hearing. Elife 9, e51419.
Peelle, J.E., 2012. The hemispheric lateralization of speech processing depends on what "speech" is: a hierarchical perspective. Front. Media SA 309.
Petersen, E.B., Wöstmann, M., Obleser, J., Lunner, T., 2017. Neural tracking of attended versus ignored speech is differentially affected by hearing loss. J. Neurophysiol. 117, 18–27.
Ponton, C.W., Vasama, J.-P., Tremblay, K., Khosla, D., Kwong, B., Don, M., 2001. Plasticity in the adult human central auditory system: evidence from late-onset profound unilateral deafness. Hear. Res. 154, 32–44.
Presacco, A., Simon, J.Z., Anderson, S., 2016. Evidence of degraded representation of speech in noise, in the aging midbrain and cortex. J. Neurophysiol. 116, 2346–2355.
Puschmann, S., Daeglau, M., Stropahl, M., Mirkovic, B., Rosemann, S., Thiel, C.M., Debener, S., 2019. Hearing-impaired listeners show increased audiovisual benefit when listening to speech in noise. Neuroimage 196, 261–268.
Reetzke, R., Gnanateja, G.N., Chandrasekaran, B., 2021. Neural tracking of the speech envelope is differentially modulated by attention and language experience. Brain Lang. 213, 104891.
Rimmele, J.M., Golumbic, E.Z., Schröger, E., Poeppel, D., 2015. The effects of selective attention and speech acoustics on neural speech-tracking in a multi-talker scene. Cortex 68, 144–154.
Sanes, D.H., 2013. Synaptic and cellular consequences of hearing loss. Deafness 129–149.
Scheffler, K., Bilecen, D., Schmid, N., Tschopp, K., Seelig, J., 1998. Auditory cortical responses in hearing subjects and unilateral deaf patients as detected by functional magnetic resonance imaging. Cerebral Cortex (New York, NY: 1991) 8, 156–163.
Shang, Y., Hinkley, L.B., Cai, C., Mizuiri, D., Cheung, S.W., Nagarajan, S.S., 2020. Cross-modal plasticity in adult single-sided deafness revealed by alpha band resting-state functional connectivity. Neuroimage 207, 116376.
Sharma, A., Glick, H., Campbell, J., Torres, J., Dorman, M., Zeitler, D.M., 2016. Cortical plasticity and reorganization in pediatric single-sided deafness pre-and postcochlear implantation: a case study. Otol. Neurotol. 37, e26–e34.
Sohal, V.S., Rubenstein, J.L., 2019. Excitation-inhibition balance as a framework for investigating mechanisms in neuropsychiatric disorders. Mol. Psychiatry 24, 1248–1257.
Sprekeler, H., 2017. Functional consequences of inhibitory plasticity: homeostasis, the excitation-inhibition balance and beyond. Curr. Opin. Neurobiol. 43, 198–203.
Su, M., Ren, F., Li, N., Li, F., Zhao, M., Hu, X., Edden, R.A., Li, M., Li, X., Gao, F., 2024. Alterations of Excitation–Inhibition Balance and Brain Network Dynamics Support Sensory Deprivation Theory in Presbycusis. Hum. Brain Mapp. 45, e70067.
Takesian, A.E., Kotak, V.C., Sanes, D.H., 2009. Developmental hearing loss disrupts synaptic inhibition: implications for auditory processing. Future Neurol. 4, 331–349.
Takesian, A.E., Kotak, V.C., Sanes, D.H., 2012. Age-dependent effect of hearing loss on cortical inhibitory synapse function. J. Neurophysiol. 107, 937–947.
Tao, H.W., Li, Y.-t., Zhang, L.I., 2014. Formation of excitation-inhibition balance: inhibition listens and changes its tune. Trends. Neurosci. 37, 528–530.
Tervaniemi, M., Hugdahl, K., 2003. Lateralization of auditory-cortex functions. Brain Res. Rev. 43, 231–246.
Turrigiano, G., 2012. Homeostatic synaptic plasticity: local and global mechanisms for stabilizing neuronal function. Cold. Spring. Harb. Perspect. Biol. 4 a005736.
Turrigiano, G.G., Nelson, S.B., 2004. Homeostatic plasticity in the developing nervous system. Nat. Rev. Neurosci. 5, 97–107.
Van Hirtum, T., Somers, B., Dieudonné, B., Verschueren, E., Wouters, J., Francart, T., 2023. Neural envelope tracking predicts speech intelligibility and hearing aid benefit in children with hearing loss. Hear. Res. 439, 108893.
Verschueren, E., Gillis, M., Decruy, L., Vanthornhout, J., Francart, T., 2022. Speech understanding oppositely affects acoustic and linguistic neural tracking in a speech rate manipulation paradigm. J. Neurosci. 42, 7442–7453.
Voytek, B., Kramer, M.A., Case, J., Lepage, K.Q., Tempesta, Z.R., Knight, R.T., Gazzaley, A., 2015. Age-related changes in 1/f neural electrophysiological noise. J. Neurosci. 35, 13257–13265.
Wang, Y., Wu, D., Ding, N., Zou, J., Lu, Y., Ma, Y., Zhang, X., Yu, W., Wang, K., 2025. Linear phase property of speech envelope tracking response in Heschl's gyrus and superior temporal gyrus. Cortex 186, 1–10.
Yizhar, O., Fenno, L.E., Prigge, M., Schneider, F., Davidson, T.J., O'Shea, D.J., Sohal, V. S., Goshen, I., Finkelstein, J., Paz, J.T., Stehfest, K., Fudim, R., Ramakrishnan, C., Huguenard, J.R., Hegemann, P., Deisseroth, K., 2011. Neocortical excitation/inhibition balance in information processing and social dysfunction. Nature 477, 171–178.
Zou, J., Feng, J., Xu, T., Jin, P., Luo, C., Zhang, J., Pan, X., Chen, F., Zheng, J., Ding, N., 2019. Auditory and language contributions to neural encoding of speech features in noisy environments. Neuroimage 192, 66–75.